Synthesis, Structure, and Physical Properties of the Bis(7,7,8,8-tetracyano-*p*-quinodimethane) Salt of the Paramagnetic Cluster Tris[(di-μ-chloro)(hexamethylbenzene)niobium], $[Nb_3(\mu\text{-}Cl)_6(C_6Me_6)_3]^{2+}(TCNQ)_2^{2-}$

Stephen Z. Goldberg,[1a] Bruce Spivack,[1a] George Stanley,[1a] Richard Eisenberg,*[1a] David M. Braitsch,[1a] Joel S. Miller,*[1b] and Martin Abkowitz[1b]

Contribution from the Department of Chemistry, University of Rochester, Rochester, New York 14627, and the Physical and Chemical Sciences Laboratory, Webster Research Center, Xerox Corporation, Rochester, New York 14644.
Received June 1, 1976

Abstract: The title complex has been synthesized from the reaction of $Nb_3Cl_6(C_6Me_6)_3^+PF_6^-$, Li^+TCNQ^-, and TCNQ in acetonitrile. Its crystal and molecular structures have been determined from three-dimensional x-ray data obtained by counter techniques. The complex crystallizes in the monoclinic space group $P2_1/m$ with two formula units per unit cell. Cell dimensions are: a = 8.838 (3), b = 27.201 (7), c = 12.868 (3) Å, β = 90.96 (2)°, and V = 3092.9 (15) Å^3. The conventional and weighted R factors for refinement on F at convergence for 2172 reflections with $F_o^2 \geq 3\sigma(F_o^2)$ and $2\theta \leq 45°$ are 0.053 and 0.065. The crystal structure consists of zigzag chains of alternating di-μ-chloro-(hexamethylbenzene)niobium trimer cations and TCNQ anion dimers. The trinuclear cluster has m symmetry with two crystallographically independent Nb–Nb distances of 3.327 (2) and 3.344 (3) Å. There is one crystallographically independent TCNQ anion which forms a dimeric unit with its centrosymmetrically related form. The interplanar spacing between TCNQ moieties is 3.10 Å and the overlap between them is of an exo double bond ring type. The mean separation of 3.65 Å between the slightly bent hexamethylbenzene and TCNQ units suggests little interaction. The room temperature ESR spectrum consists of a nearly isotropic [g = 1.996 (2)] and relatively broad absorption [peak to peak derivative line width of 36.95 (3) Oe]. This is consistent with the unpaired electron residing on the niobium cluster. Thus, the molecule is $[Nb_3Cl_6(C_6Me_6)_3]^{2+}(TCNQ)_2^{2-}$ and represents the solid-state stabilization of the previously postulated $S = \frac{1}{2}$ cluster by TCNQ. The single-crystal and polycrystalline conductivity data indicate a semiconductor behavior with a room temperature conductivity of 0.001 ohm^{-1} cm^{-1} and an activation energy of 0.35 eV (2800 cm^{-1}).

With the observation of a one-dimensional (1-D) metallic state in both inorganic[2-4] and organic complexes[3-6] there has been an increased emphasis on the synthesis and characterization of new highly conducting inorganic[7] and organic[6] one-dimensional complexes. To date the most successful systems for effecting the formation of a highly conducting one-dimensional chain are based on tetracyanoplatinate moieties[2-4,7] and on charge-transfer complexes of 7,7,8,8-tetracyano-*p*-quinodimethane, TCNQ.[3-6] In terms of the current understanding of the physics of 1-D complexes, a variety of factors are significant in the design of a highly conducting system. The choice of counterion is extremely important. The symmetry, polarizability, and size of the counterion are major considerations in the design of new highly conducting systems.[6] The symmetry of the counterion increases the probability of the formation of a uniform chain and its polarizability provides a medium for the stabilization of a metallic state.[2,6] The latter is the basis for Little's exciton theory for stabilization of a superconducting state at room temperature.[8,9] Garito and Heeger have stated[6] regarding the stabilization of a metallic state that "*Molecular design should be dominated by attempts to obtain maximum polarizability with minimum size.*"

For the organic 1-D systems based on TCNQ a variety of planar organic cations have been used to stabilize a metallic state. In addition to these open-[5,6] and closed-shell[10-13] organic cations, a variety of organometallic cations have been used. For example, $(\eta^5\text{-}C_5H_5)_2Fe^+$,[11a] bis(fulvalene)diiron$^+$,[11b] and $(\eta^6\text{-}C_7H_8)_2Cr^+$[14] form 1:2 salts with TCNQ which have been characterized by high conductivity at room temperature. Based on these considerations we attempted to prepare the TCNQ complex salt of the symmetrical $[Nb_3Cl_6(C_6Me_6)_3]^+$ cation.[14-17] It was hoped that the symmetry of the cation would permit the formation of a 1-D chain of TCNQ moieties as observed for the other cations, such as $(\eta^6\text{-}C_7H_8)_2Cr(TCNQ)_2$.[13a] In addition it was thought that the polarizability of the niobium cluster cation would aid in the formation of a complex TCNQ salt with high conductivity.

An alternative possibility which seemed plausible was that in solution TCNQ would oxidize the diamagnetic trimer monocation to the diamagnetic hexamer tetracation,[15-16]

$$2Nb_3Cl_6(C_6Me_6)_3^+ + 2TCNQ \rightarrow 2TCNQ^- + Nb_6Cl_{12}(C_6Me_6)_6^{4+} \quad (1)$$

and subsequently form a complex TCNQ salt.

$$Nb_6Cl_{12}(C_6Me_6)_6^{4+} + 4TCNQ^- + xTCNQ \rightarrow Nb_6Cl_{12}(C_6Me_6)_6(TCNQ)_{4+x} \quad (2)$$

Neither of these possibilities was realized in the present study, but a more intriguing structural result emerged. In this study the trimer is oxidized to the $S = \frac{1}{2}$ dication, which is stabilized in the solid state by dimeric TCNQ units in an unusual zigzag arrangement. The TCNQ dimers exhibit a seemingly tight interaction between adjacent anions, and the paramagnetic Nb trimer, which had previously been postulated[16] as an intermediate in the cluster oxidation and dimerization, provides an interesting comparison with the structurally known diamagnetic $[Nb_3(\mu\text{-}Cl)_6(C_6Me_6)_3]^+$ system.[14]

Experimental Section

Preparation of Samples. Commercially available TCNQ and LiTCNQ[11] were recrystallized from commercial acetonitrile of satisfactory purity.[11] A hot filtered acetonitrile solution (60 ml) of 59.75 mg of $[Nb_3Cl_6(C_6Me_6)_3]PF_6$[16] (0.061 mmol) was added to a hot filtered acetonitrile solution containing 34.10 mg of LiTCNQ[11] (0.162 mmol) and 13.90 mg of TCNQ (0.068 mol). The solution was cooled to −8 °C and after 24 h at this temperature dark purple homogeneous crystals separated and were collected (35.2 mg; 0.025 mmol; 40%).

Table I. Positional and Thermal Parameters for $[Nb_3Cl_3(C_6Me_6)_3](TCNQ)_2$

Atom	x	y	z	β_{11}[a]	β_{22}	β_{33}	β_{12}	β_{13}	β_{23}
Nb(1)	0.41310 (20)[b]	0.25	−0.11447 (14)	74.6 (29)	9.1 (3)	38.8 (14)	0	0.5 (16)	0
Nb(2)	0.27875 (14)	0.31146 (5)	0.08756 (10)	71.8 (18)	8.18 (20)	38.9 (9)	0.0 (6)	−2.0 (10)	−0.9 (4)
Cl(1)	0.0712 (6)	0.25	0.1021 (4)	78. (8)	9.4 (9)	64. (5)	0	2. (5)	0
Cl(2)	0.3989 (6)	0.25	0.2085 (4)	108. (9)	12.0 (9)	41. (4)	0	−16. (5)	0
Cl(3)	0.5331 (4)	0.31066 (13)	0.00562 (27)	84. (5)	11.1 (6)	53.5 (26)	−3.5 (16)	3. (3)	−4.6 (12)
Cl(4)	0.2043 (4)	0.31107 (14)	−0.09951 (25)	98. (5)	12.1 (6)	40.3 (25)	6.3 (17)	−7.7 (29)	−0.1 (11)
C(1)	0.0872 (17)	0.3671 (5)	0.1036 (12)	141. (27)	6.1 (23)	69. (13)	0. (7)	47. (15)	0. (4)
C(2)	0.2027 (16)	0.3977 (5)	0.0566 (11)	115. (25)	6.1 (23)	63. (12)	7. (6)	6. (15)	−7. (4)
C(3)	0.3526 (17)	0.3992 (5)	0.1016 (11)	136. (27)	8.6 (24)	55. (12)	7. (7)	4. (15)	−4. (5)
C(4)	0.3840 (16)	0.3697 (5)	0.1943 (11)	112. (25)	10.2 (25)	54. (12)	−2. (7)	11. (14)	−2. (5)
C(5)	0.2609 (17)	0.3539 (5)	0.2586 (11)	99. (26)	10.4 (25)	66. (13)	−5. (6)	−8. (15)	−4. (5)
C(6)	0.1141 (18)	0.3531 (5)	0.2123 (12)	167. (31)	10.0 (26)	73. (14)	9. (7)	42. (17)	−8. (5)
C(7)	−0.0733 (16)	0.3671 (6)	0.0564 (12)	81. (24)	24. (4)	89. (14)	−14. (8)	−63. (15)	10. (6)
C(8)	0.1659 (17)	0.4285 (5)	−0.0400 (11)	163. (28)	13.3 (27)	54. (12)	7. (7)	−30. (15)	10. (5)
C(9)	0.4785 (17)	0.4303 (6)	0.0510 (13)	112. (25)	13.4 (28)	103. (15)	−9. (7)	50. (16)	6. (5)
C(10)	0.5451 (16)	0.3696 (6)	0.2407 (12)	88. (25)	18. (3)	101. (15)	−5. (7)	−54. (16)	−5. (6)
C(11)	0.2858 (19)	0.3384 (6)	0.3703 (10)	225. (34)	19. (3)	25. (10)	0. (8)	−17. (15)	6. (5)
C(12)	−0.0249 (17)	0.3346 (6)	0.2765 (13)	134. (27)	16. (3)	96. (15)	−8. (8)	64. (17)	1. (5)
C(13)	0.6463 (24)	0.25	−0.1935 (16)	99. (37)	23. (5)	33. (16)	0	14. (19)	0
C(14)	0.5765 (20)	0.2050 (6)	−0.2326 (11)	175. (32)	19. (3)	39. (11)	27. (8)	41. (16)	1. (5)
C(15)	0.4328 (19)	0.2044 (6)	−0.2799 (12)	150. (30)	18. (3)	53. (12)	−2. (8)	55. (16)	0. (5)
C(16)	0.3530 (28)	0.25	−0.2892 (17)	174. (44)	19. (5)	38. (16)	0	8. (21)	0
C(17)	0.8021 (25)	0.25	−0.1444 (20)	44. (35)	72. (11)	81. (23)	0	−25. (23)	0
C(18)	0.6611 (26)	0.1560 (7)	−0.2220 (14)	434. (56)	24. (4)	85. (16)	80. (13)	29. (24)	8. (7)
C(19)	0.3623 (25)	0.1554 (6)	−0.3231 (13)	404. (51)	19. (4)	83. (16)	−38. (11)	91. (23)	−26. (6)
C(20)	0.1867 (25)	0.25	−0.3464 (24)	62. (36)	35. (7)	185. (36)	0	−60. (29)	0
C(21)	0.0102 (15)	0.4436 (5)	0.4696 (11)	67. (21)	8.7 (24)	63. (13)	−9. (6)	11. (14)	−4. (4)
C(22)	0.1695 (17)	0.4498 (5)	0.4994 (12)	124. (26)	9.9 (25)	60. (12)	3. (7)	−5. (15)	−3. (5)
C(23)	0.2676 (17)	0.4706 (5)	0.4314 (11)	144. (28)	11.6 (26)	34. (12)	6. (7)	−18. (14)	0. (4)
C(24)	0.2141 (15)	0.4869 (5)	0.3336 (12)	76. (23)	11.1 (26)	63. (13)	−4. (6)	15. (14)	−5. (5)
C(25)	0.0554 (16)	0.4825 (5)	0.3014 (12)	92. (24)	10.8 (27)	68. (13)	2. (6)	−12. (15)	−8. (5)
C(26)	−0.0447 (17)	0.4600 (5)	0.3688 (11)	136. (27)	10.0 (24)	46. (12)	3. (7)	−10. (15)	0. (4)
C(27)	−0.0882 (17)	0.4194 (5)	0.5389 (12)	96. (24)	12.5 (26)	54. (12)	−2. (7)	−3. (14)	0. (5)
C(28)	0.3130 (17)	0.5073 (6)	0.2608 (12)	103. (26)	14.6 (28)	55. (12)	9. (7)	−9. (15)	−3. (5)
C(29)	−0.2377 (22)	0.4110 (6)	0.5137 (13)	153. (31)	19. (3)	60. (14)	−8. (9)	0. (17)	10. (6)
C(30)	−0.0387 (17)	0.4014 (6)	0.6378 (14)	97. (27)	17. (3)	76. (15)	4. (7)	−5. (17)	6. (6)
C(31)	0.4738 (21)	0.5133 (6)	0.2827 (13)	155. (31)	16. (3)	67. (14)	1. (9)	−8. (18)	1. (5)
C(32)	0.2646 (17)	0.5257 (6)	0.1636 (13)	101. (26)	14. (3)	72. (15)	7. (7)	29. (16)	11. (5)
N(1)	−0.3656 (17)	0.4025 (6)	0.4962 (12)	195. (31)	32. (4)	92. (14)	−19. (10)	−21. (18)	6. (6)
N(2)	0.0023 (17)	0.3887 (6)	0.7168 (13)	183. (29)	27. (4)	113. (16)	−9. (8)	−27. (18)	22. (6)
N(3)	0.5989 (15)	0.5168 (7)	0.2988 (12)	93. (23)	40. (4)	108. (15)	1. (9)	−15. (16)	1. (7)
N(4)	0.2278 (15)	0.5400 (5)	0.0841 (12)	161. (27)	18.1 (29)	93. (14)	2. (7)	21. (16)	10. (5)
Me(1)[c]	0.832 (5)	0.25	0.511 (3)	18.4 (14)[d]					
Me(2)	0.661 (5)	0.25	0.479 (3)	18.8 (14)					

[a] The form of the anisotropic thermal ellipsoid is $\exp[-(h^2\beta_{11} + k^2\beta_{22} + l^2\beta_{33} + 2hk\beta_{12} + 2hl\beta_{13} + 2kl\beta_{23})]$. Anisotropic thermal parameters have multiplied by 10^4. [b] In this and subsequent tables the estimated standard deviations of the least significant figures are given in parentheses. [c] Me represents an atom of the solvent molecule refined as 50% C and 50% O. [d] Isotropic temperature factor, B, in the expression $\exp[\beta \cdot ((\theta)/\lambda)^2]$.

Large single crystals were grown by maintaining the filtrate at −8 °C for extended periods of time. Anal. Calcd[18] for $[Nb_3Cl_6(C_6(CH_3)_6)_3](C_{12}H_4N_4)_2 \cdot H_3CCN$: C, 52.16; H, 4.59; N, 8.83; Cl, 14.90. Found: C, 51.98, 52.35; H, 4.60, 4.59; N, 8.77, 8.73; Cl, 14.82, 15.19.

Instrumentation. Two probe polycrystalline conductivity measurements were made with a Triplet 801 VOM meter. Four probe single-crystal conductivity measurements were made with a Keithly 225 current source, Model 180 nanovoltmeter, and a Model 616 electrometer. Temperature control was provided by a Delta oven. Differential scanning calorimetry was done with a du Pont 900 thermal analyzer. ESR measurements were performed using a 3-cm homodyne four-crystal balanced-bridge instrument. Two crystals were used to derive an FM discriminator wave form, which kept the klystron dc phase locked to the experimental cavity. This assured that the signal detected contained no dispersive component and that the absorption shape was faithfully reproduced. Magnetic susceptibility was determined by a comparison of the ESR spectrum with that of a Varian 1% pitch in KCl (g = 2.0028) containing 3×10^{15} spins per inch as calibrant. A dual sample cavity was employed and the polycrystalline samples were degassed.

Collection and Reduction of the Single-Crystal X-Ray Data. Single crystals of $[Nb_3Cl_6(C_6Me_6)_3](TCNQ)_2$ suitable for a diffraction study were obtained as described above. The space group and preliminary lattice constants were determined from oscillation, Weissenberg, and precession photographs. The Laue symmetry was $2/m$ and the only systematic absence was for $0k0$ with k odd. These conditions limit the possible space groups to $P2_1$ and $P2_1/m$.[19] Precise cell constants at 20 °C were determined from a least-squares refinement[20] of the setting angles of 12 well-resolved reflections ($(\sin\theta)/\lambda > 0.36$), which were carefully centered (using Mo $K\alpha_1$ radiation, λ = 0.709261 Å) on a Picker FACS-1 diffractometer equipped with a graphite monochromator. The lattice constants are a = 8.838 (3), b = 27.201 (7), c = 12.868 (3) Å, β = 90.96 (2)°, V = 3092.9 (15) Å.^{3}

The experimental density of 1.51 (2) g/cm^3 as determined by flotation in CH_2Cl_2–CCl_4 was in good agreement with the value of 1.49 g/cm^3 calculated for two formula units of $[Nb_3Cl_6(C_6Me_6)_3](TCNQ)_2$ per unit cell. It should be noted, however, that the calculated densities based on one solvent molecule of crystallization were 1.52 and 1.53 g/cm^3 for CH_3OH and CH_3CN, respectively; thus no conclusions regarding the possible presence and nature of a solvent molecule could be drawn at this stage (vide infra).

Intensity data were collected using the same crystal which was used

for the determination of the space group and lattice constants. The crystal dimensions were approximately 0.4 × 0.10 × 0.06 mm and the crystal was mounted so that the a^* axis was nearly parallel to the ϕ axis of the diffractometer (the a axis was coincident with the long axis of the crystal). Mosaic spread was checked by means of narrow source, open counter ω scans.[21] Full widths at half maximum for some typical strong reflections were in the range of 0.06–0.12°.

Intensities were measured by the θ–2θ scan technique. The takeoff angle for the x-ray tube was set at 1.9°, so that intensities of typical strong reflections were ~80% of their maximum value as a function of takeoff angle. Data were collected at a scan rate of 1°/min with scans being made from 0.7° below the $K\alpha_1$ peak to 0.7° above the $K\alpha_2$ peak. Attenuator foils were automatically inserted when the intensity of the diffracted beam reached 10 000 Hz. The pulse height analyzer was set for a 90% window centered on the Mo $K\bar{\alpha}$ radiation.

Data were collected for the quadrant with $k \geq 0$ and $l \geq 0$ for $3° \leq 2\theta \leq 45°$. Three standard reflections were monitored after every 50 observations. The standards showed no decay during data collection. A total of 4389 reflections were observed, of which 208 with $l = 0$ were observed as Friedel pairs. The values of I and $\sigma^2(I)$ were obtained using the expressions previously described.[22,23] The value of p used in the expression for the variance was chosen as 0.04. Values of I and $\sigma^2(I)$ were converted to F^2 and $\sigma^2(F^2)$ by application of Lorentz and polarization corrections.[24] Of the 14 systematically absent reflections, none had $F^2 > 1.4\sigma(F^2)$. Two low-angle reflections were rejected because of their nearness to the beam. The absorption coefficient for Mo $K\bar{\alpha}$ radiation is 8.37 cm^{-1} and no correction for absorption was made on the the assumption that the correct space group was $P2_1/m$, the Friedel pairs were averaged. The R factor for averaging was 3.6%. The final data set consisted of 4165 independent reflections, of which only the 2172 with $F_o^2 \geq 3\sigma(F_o^2)$ were used in the refinement of the structure.

Solution and Refinement of the Structure. The structure was solved and refined using standard Patterson, Fourier, and least-squares methods.[24] In all least-squares refinements the quantity minimized was $\Sigma w(|F_o| - |F_c|)^2$, where the weights, w, were taken as $(1/\sigma(F^2)) = 4F_o^2/\sigma^2(F_o^2)$. The atomic scattering factors for neutral Nb, Cl, O, N, and C were taken from the tabulation of Cromer and Mann.[25] Corrections for anomolous dispersion of Nb and Cl were made using the $\Delta f'$ and $\Delta f''$ values of Cromer and Lieberman.[26]

A three-dimensional Patterson map could be interpreted in terms of the centric $P2_1/m$ space group and the successful refinement of the structure confirmed this choice. The positions of two crystallographically independent Nb atoms, one at a general position (4f) and one on the mirror plane (2e), were deduced from the Patterson map. Refinement of the scale factor, positional, and isotropic thermal parameters yielded $R_1 = 0.38$, $R_2 = 0.45$.[27] A difference Fourier map phased by this model revealed the positions of the four crystallographically independent Cl atoms, two at general positions and two on the mirror plane. A second difference map, this one phased by the six atom model, revealed the positions of all the carbon and nitrogen atoms of the TCNQ and hexamethylbenzene molecules. Refinement of a model containing 42 isotropically treated atoms resulted in $R_1 = 0.07$ and $R_2 = 0.10$. A model in which all atoms were treated anisotropically refined to $R_1 = 0.060$ and $R_2 = 0.084$.

A difference map computed at this point showed as its most prominent features two peaks on the mirror plane. The peaks were within bonding distance of each other, but were well separated from the atoms already included in the model. At the time the structure was solved it was erroneously thought that methanol was used during the preparation of the compound. Based on this belief, a model involving isotropic refinement of two atoms, each with a scattering factor curve corresponding to the average of those for C and O was used. Refinement to convergence yielded values of 0.053 and 0.065, respectively, for R_1 and R_2. On the final cycle of refinement no parameter shifted by more than 2% of its estimated standard deviation. A final difference Fourier map showed no peaks larger than 1.5 $e^-/Å^3$ or 20% of the height of a typical carbon atom in this structure. This map did not reveal positions for the hydrogen atoms, so at this point the refinement was considered to be complete. The error in an observation of unit weight[27] was 1.90 e^- for 2172 reflections and 364 variables. The quantity $\Sigma w(|F_o| - |F_c|)^2$ showed no trends as a function of $|F_o|$, but it did increase for small values of $(\sin\theta)/\lambda$. After completion of the refinement it became clear that methanol had never been introduced into the system and that the crystallographic model was chemically unrealistic. If the molecule of a crystallization is in fact acetonitrile, then it is disordered over two or more positions such that reinforcement occurs at only two atomic sites. Since all other structural parameters were insensitive to inclusion of the solvent molecule in the model, no attempt was made to refine a new model with acetonitrile as the solvent molecule.

The positional and thermal parameters obtained from the final cycle of the least-squares refinement are presented in Table I. A listing of the observed and calculated structure factors for those reflections used in the refinement is available.[28]

Description of Structure

The structure consists of the packing of di-μ-chloro(hexamethylbenzene)niobium trimer cations, TCNQ anion dimers, and solvent molecules of crystallization. The assignment of charges to the cationic and anionic species will be considered below. The overall structural arrangement is novel, with strongly bonded TCNQ dimers interacting with hexamethylbenzene of the niobium cluster to give a zigzag chain as illustrated in Figure 1. A view showing the relationship of this chain to the crystallographic unit cell is presented in Figure 2. Distances, angles, and root mean square amplitudes of vibration are presented in Tables II–IV.

Table II. Distances for $[Nb_3Cl_6(C_6Me_6)_3](TCNQ)_2$

Atoms	Distance, Å	Atoms	Distance, Å
Nb(1)-Nb(2)	3.327 (2)	C(13)-C(17)	1.505 (29)
Nb(2)-Nb(2)	3.344 (3)	C(14)-C(18)	1.534 (21)
Av[a]	3.335 (9)	C(15)-C(19)	1.569 (21)
		C(16)-C(20)	1.633 (31)
		Av	1.560 (28)
Nb(1)-Cl(3)	2.486 (4)		
Nb(1)-Cl(4)	2.492 (4)	Nb(2)-C(1)	2.282 (14)
Nb(2)-Cl(1)	2.491 (4)	Nb(2)-C(2)	2.470 (14)
Nb(2)-Cl(2)	2.508 (4)	Nb(2)-C(3)	2.481 (14)
Nb(2)-Cl(3)	2.499 (3)	Nb(2)-C(4)	2.285 (14)
Nb(2)-Cl(4)	2.485 (3)	Nb(2)-C(5)	2.492 (15)
Av	2.494 (3)	Nb(2)-C(6)	2.461 (14)
		Nb(1)-C(13)	2.313 (20)
		Nb(1)-C(14)	2.443 (14)
C(1)-C(2)	1.456 (18)	Nb(1)-C(15)	2.472 (15)
C(2)-C(3)	1.438 (18)	Nb(1)-C(16)	2.302 (23)
C(3)-C(4)	1.461 (19)		
C(4)-C(5)	1.444 (19)	C(21)-C(22)	1.463 (19)
C(5)-C(6)	1.419 (19)	C(21)-C(26)	1.447 (18)
C(6)-C(1)	1.465 (20)	C(23)-C(24)	1.409 (18)
Av	1.447 (7)	C(24)-C(25)	1.461 (18)
		Av	1.445 (12)
C(1)-C(7)	1.533 (19)	C(22)-C(23)	1.365 (18)
C(2)-C(8)	1.530 (19)	C(25)-C(26)	1.391 (18)
C(3)-C(9)	1.549 (19)	Av	1.378 (13)
C(4)-C(10)	1.535 (19)		
C(5)-C(11)	1.510 (18)	C(21)-C(27)	1.418 (18)
C(6)-C(12)	1.574 (20)	C(24)-C(28)	1.405 (18)
Av	1.539 (9)	Av	1.412 (7)
		C(27)-C(29)	1.374 (20)
C(13)-C(14)	1.456 (19)	C(27)-C(30)	1.425 (20)
C(14)-C(15)	1.399 (21)	C(28)-C(31)	1.453 (21)
C(15)-C(16)	1.431 (18)	C(28)-C(32)	1.406 (20)
Av	1.429 (16)	Av	1.415 (17)
		C(29)-N(1)	1.171 (19)
C(1)-C(4)	2.854 (22)	C(30)-N(2)	1.128 (18)
C(2)-C(5)	2.897 (21)	C(31)-N(3)	1.126 (18)
C(3)-C(6)	2.855 (21)	C(32)-N(4)	1.137 (17)
C(13)-C(16)	2.850 (32)	Av	1.141 (11)
C(14)-C(15)	2.833 (20)		
Av	2.858 (11)	Me(1)-Me(2)	1.56 (5)

[a] Average values are computed as $\bar{x} = (\Sigma x_i)/n$ and $\sigma(\bar{x}) =](\Sigma(x_i - \bar{x})^2)/n(n-1)]^{1/2}$, where n is the number of chemically equivalent values.

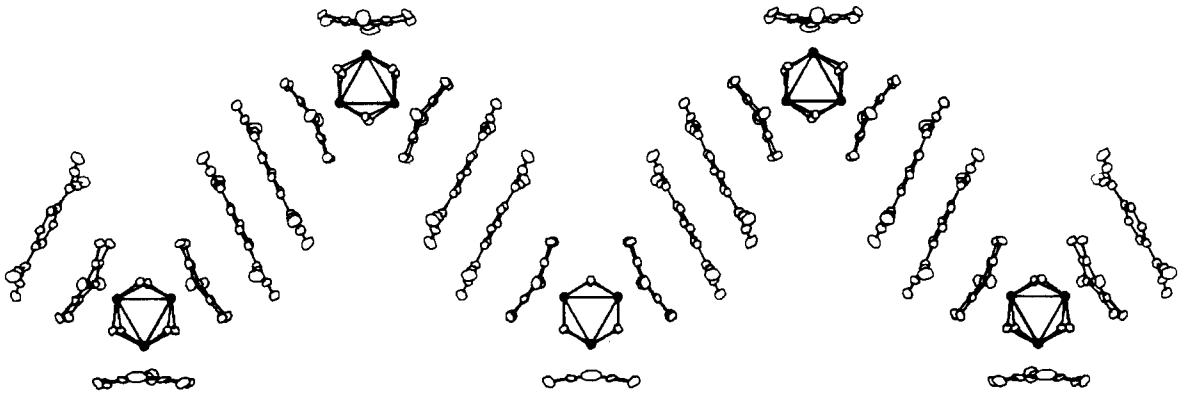

Figure 1. The zigzag chain of cations and anions. The *b* axis is horizontal. The three trimers at the bottom of the illustration are in the plane of the paper, while the two trimers at the top are below the plane.

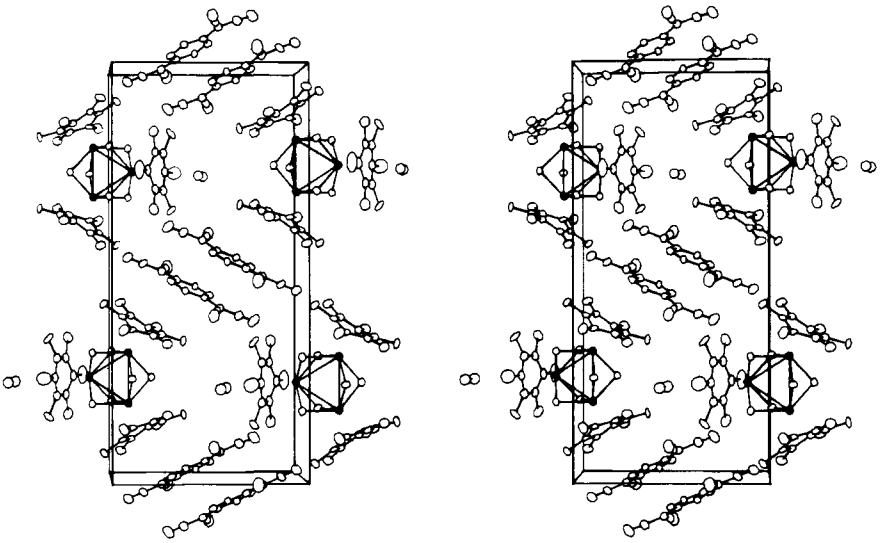

Figure 2. A stereoscopic drawing of the unit cell of $[Nb_3Cl_6(C_6Me_6)_3](TCNQ)_2$. The *a* axis is horizontal and the *b* axis is vertical.

Di-μ-chloro-(hexamethylbenzene)niobium Trimer. The choice of the niobium cluster as a counterion for TCNQ was based on the fact that the trimeric cluster is symmetrical, polarizable, and capable of undergoing facile oxidation and dimerization. In the present case the cation is trinuclear (Figure 3) and possesses crystallographic mirror symmetry. The two independent Nb–Nb distances are 3.327 (2) and 3.344 (3) Å, with the mean being 3.335 (9) Å. This value is in agreement with a value of 3.334 (6) Å found by Churchill and Chang[14] in $[Nb_3Cl_6(C_6Me_6)_3]Cl$. The difference between the two Nb–Nb distances determined in this work is, however, greater than 5σ and may well indicate a small distortion from an equilateral triangle as a result of the one-electron oxidation. In their study, Churchill and Chang[14] observed Nb–Cl distances of 2.466 (8) and 2.499 (9) Å. In the present study the distances to the bridging Cl atoms range from 2.485 (3) to 2.508 (4) Å, with the mean being 2.494 (3) Å. Thus, in both studies, the chloro bridges are symmetrical.

There are two crystallographically independent hexamethylbenzene ligands in the cluster; one is located in a general position, whereas the second has its center on the mirror plane and is oriented normal to the plane. Both molecules are slightly bent, as is evident from the least-squares planes presented in Table V. A similar bending seems to be present in $[Nb_3Cl_6(C_6Me_6)_3]Cl$, but was not discussed in detail because of a crystallographic disorder present in that structure.[14] However, in hexamethylbenzene[29] and in some complexes containing hexamethybenzene[30-32] the molecule is planar. The distortions from planarity observed in the present cluster apparently are the result of steric rather than electronic factors as observed for $(C_6Me_6)_2Ru$.[31] The mean C–C bonds within the rings are 1.447 (7) and 1.429 (16) Å for the hexamethylbenzenes occupying general and special positions, respectively. In $Cr(CO)_3(C_6Me_6)$[30] and $(C_6Me_6)_2Ru$[31] the C–C ring distances are 1.417 (15) and 1.410 (4) Å, respectively, and in the charge-transfer complex between TCNQ and hexamethylbenzene the average C–C ring distance is 1.405 (2) Å.[32] Trans distances within the benzene rings (Table II) show no evidence of a Dewar benzene-type structure. The distances to the methyl groups are also normal, with the mean value for the general and special molecules being 1.539 (9) and 1.560 (28) Å, respectively. The thermal ellipsoids for each hexamethylbenzene are consistent with the dominant thermal motion being a librational motion about an axis passing through the niobium and the center of the ring. Atom C(20) is anomalous with respect to both the shape of its thermal ellipsoid and its long distance from C(16) (1.633 (31) Å).

The hexamethylbenzene molecules coordinate as η^6 ligands. For each molecule there are two short and four long Nb–C contacts, which is consistent with the slight bending observed for the arene system. The planes of the arenes are nearly normal to the plane of the metal trimer, the dihedral angles being 89.4° for both hexamethylbenzene molecules. The angle between the planes of the two arene systems is 60.3°.

TCNQ Anion. The structure of an individual TCNQ species is shown in Figure 4, and the overlap between the two molecules forming a tight dimer is presented in Figure 5. The dimer possesses a dinegative charge in the present structure and the

Table III. Selected Bond Angles for $[Nb_3Cl_6(C_6Me_6)]_3(TCNQ)_2$

Atoms	Angle, deg	Atoms	Angle, deg
Nb(1)-Nb(2)-Nb(2)	59.83 (3)	C(27)-C(21)-C(22)	119.1 (14)
Nb(2)-Nb(1)-Nb(2)	60.34 (6)	C(27)-C(21)-C(26)	120.5 (14)
Av[a]	60.1 (3)	C(28)-C(24)-C(23)	121.2 (13)
		C(28)-C(24)-C(25)	116.6 (14)
Nb(2)-Cl(1)-Nb(2)	84.30 (17)	Av	119.3 (10)
Nb(2)-Cl(2)-Nb(2)	83.62 (16)		
Nb(1)-Cl(3)-Nb(2)	83.72 (12)	C(21)-C(27)-C(29)	121.7 (15)
Nb(1)-Cl(4)-Nb(2)	83.88 (11)	C(21)-C(27)-C(30)	122.6 (15)
Av	83.88 (15)	C(24)-C(28)-C(31)	122.1 (14)
		C(24)-C(28)-C(32)	123.4 (14)
		Av	122.4 (4)
C(21)-C(22)-C(23)	119.9 (14)		
C(22)-C(23)-C(24)	119.8 (14)	C(29)-C(27)-C(30)	115.7 (14)
C(24)-C(25)-C)26)	118.5 (14)	C(31)-C(28)-C(32)	114.5 (14)
C(25)-C(26)-C(21)	119.2 (13)	Av	115.1 (6)
Av	119.4 (3)		
		C(27)-C(29)-N(1)	176.9 (19)
		C(27)-C(30)-N(2)	177.6 (20)
C(22)-C(21)-C(26)	120.4 (13)	C(28)-C(31)-N(3)	178.3 (20)
C(23)-C(24)-C(25)	122.2 (14)	C(28)-C(32)-N(4)	178.6 (17)
Av	121.3 (9)	Av	177.9 (4)

[a] See footnote in Table II.

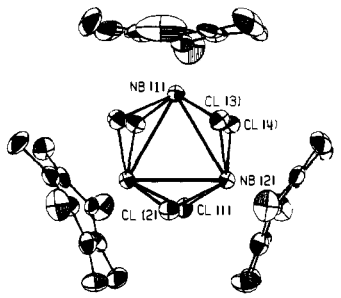

Figure 3. The $[Nb_3Cl_6(C_6Me_6)_3]^{2+}$ cation (50% probability ellipsoids).

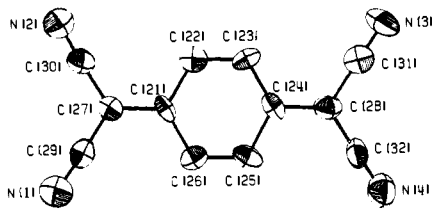

Figure 4. An individual $TCNQ^-$ molecule (50% probability ellipsoids).

molecular parameters for TCNQ are in slightly better agreement with the value obtained for $TCNQ^-$ than with those for $TCNQ^{1/2-}$.[22,23-35] The differences are very slight, however, and point out the difficulty of quantitatively correlating charge and bond lengths in these systems.

The structure reported here is unusual in that there are dimeric TCNQ groups well separated from all other TCNQ molecules. Among TCNQ structures reported to date, only two other systems contain such isolated dimers, i.e., $[Me_3NH]_2(TCNQ)_3$[36a] and benzimidazolium TCNQ.[36b] There are systems[12] in which, within a stack of TCNQ molecules, there are unequal spacings resulting in the formation of dimers such as in Rb^+TCNQ^-, where the interplanar distance within the dimer is 3.149 Å.[34] In the present study, crystallographic symmetry requires that the TCNQ rings be parallel to one another with an interplanar distance of 3.10 Å. The cyano

Table IV. Root Mean Square Amplitudes of Vibration (Å × 10^3)[a]

Atom	Minimum	Intermediate	Maximum
Nb(1)	172 (3)	181 (3)	185 (3)
Nb(2)	167 (2)	174 (2)	184 (2)
Cl(1)	175 (9)	188 (9)	233 (8)
Cl(2)	167 (9)	212 (8)	222 (8)
Cl(3)	175 (6)	191 (6)	228 (6)
Cl(4)	172 (6)	194 (6)	226 (6)
C(1)	152 (28)	175 (26)	289 (22)
C(2)	123 (33)	220 (24)	241 (22)
C(3)	163 (28)	221 (24)	239 (23)
C(4)	191 (25)	199 (25)	227 (24)
C(5)	173 (27)	214 (24)	242 (23)
C(6)	141 (32)	240 (24)	294 (24)
C(7)	102 (42)	263 (23)	342 (23)
C(8)	148 (31)	250 (23)	276 (22)
C(9)	149 (30)	239 (23)	317 (22)
C(10)	134 (33)	259 (23)	319 (22)
C(11)	134 (32)	272 (23)	302 (23)
C(12)	161 (29)	247 (23)	324 (22)
C(13)	153 (42)	207 (37)	296 (33)
C(14)	131 (32)	221 (25)	326 (24)
C(15)	140 (31)	256 (25)	228 (24)
C(16)	177 (38)	263 (34)	264 (34)
C(17)	117 (60)	269 (37)	520 (41)
C(18)	160 (34)	262 (25)	489 (28)
C(19)	153 (33)	257 (27)	457 (26)
C(20)	126 (55)	361 (37)	406 (38)
C(21)	135 (31)	189 (24)	242 (24)
C(22)	188 (25)	214 (25)	236 (24)
C(23)	157 (31)	203 (24)	253 (24)
C(24)	165 (26)	190 (24)	247 (23)
C(25)	177 (26)	188 (25)	260 (24)
C(26)	187 (26)	195 (25)	238 (23)
C(27)	192 (26)	213 (25)	218 (23)
C(28)	185 (27)	211 (24)	252 (24)
C(29)	197 (28)	241 (27)	292 (24)
C(30)	190 (29)	235 (26)	271 (24)
C(31)	229 (26)	246 (25)	256 (25)
C(32)	175 (28)	196 (28)	286 (24)
N(1)	250 (23)	281 (22)	368 (22)
N(2)	238 (24)	261 (22)	378 (22)
N(3)	188 (24)	304 (21)	386 (22)
N(4)	228 (23)	249 (21)	307 (21)
Me(1)	483 (19)[b]		
Me(2)	488 (19)[b]		

[a] Calculated along the principle axis of the thermal ellipsoids. [b] Atom refined isotropically.

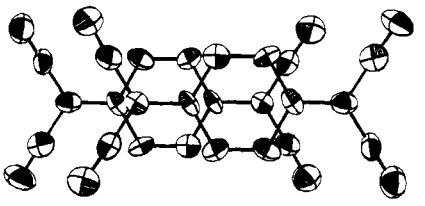

Figure 5. Overlap within the $TCNQ_2^{2-}$ dimer (50% probability ellipsoids).

groups are bent away from the neighboring TCNQ moiety. The overlap within the dimer, Figure 5, is of the symmetrical ring-exo double bond type characteristic of highly conducting TCNQ complexes[4-6] and benzimidazolium TCNQ,[36b] and is different from the ring-ring type observed in Rb^+TCNQ^-[34] and $[Me_3NH]_2(TCNQ)_3$.[36a]

Crystal Packing. As illustrated in Figures 1 and 2 the cationic and anionic species pack together to form a zigzag chain with the axis parallel to the *b* axis of the unit cell. The hexa-

Table V. Weighted Least-Squares Planes[a] Through the Six-Membered Rings of TCNQ and the Hexamethylbenzene Molecules

Atom	Deviation from plane, Å	Atom	Deviation from plane, Å
C(21)	0.000 (13)	C(1)	3.86
C(22)	−0.009 (13)	C(2)	3.57
C(23)	0.007 (14)	C(3)	3.57
C(24)	0.005 (13)	C(4)	3.88
C(25)	−0.013 (13)	C(5)	3.72
C(26)	0.011 (14)	C(6)	3.70
C(27)	0.061[b]	C(7)	3.81
C(28)	0.059	C(8)	3.24
C(29)	0.118	C(9)	3.30
C(30)	0.089	C(10)	3.95
C(31)	0.095	C(11)	3.57
C(32)	0.013	C(12)	3.57
N(1)	0.180		
N(2)	0.074		
N(3)	0.057		
N(4)	−0.001		
	$1.832x - 24.40y - 5.063z = -13.19$		
C(1)	0.161 (13)	C(7)	0.117
C(2)	−0.066 (13)	C(8)	−0.312
C(3)	−0.068 (13)	C(9)	−0.264
C(4)	0.158 (13)	C(10)	0.211
C(5)	−0.077 (14)	C(11)	−0.306
C(6)	−0.081 (14)	C(12)	−0.286
	$1.959x - 23.63y - 5.745z = -9.26$		
C(13)	−0.144 (21)	C(17)	−0.114
C(14)	0.041 (15)	C(18)	0.245
C(15)	0.036 (16)	C(19)	0.268
C(16)	−0.164 (23)	C(20)	−0.140
	$3.870x - 11.66z = 4.902$		

[a] Planes are referred to monoclinic coordinates: see W. C. Hamilton, *Acta Crystallogr.* **14**, 185 (1961). [b] Those atoms for which no estimated deviations in the distance from the plane are given were assigned zero weight in the calculation of the plane.

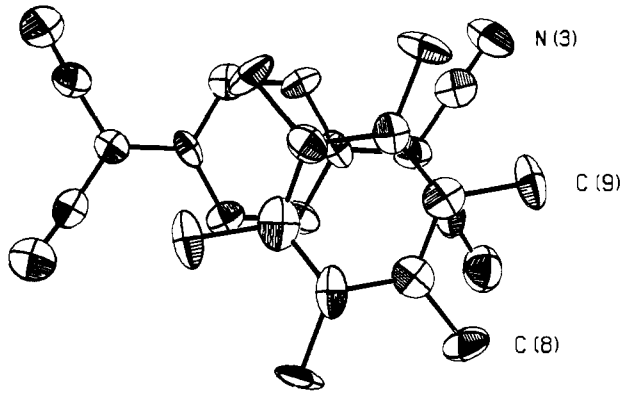

Figure 6. Interaction between the TCNQ and hexamethylbenzene moieties (50% probability ellipsoids).

methylbenzene molecule centered on the crystallographic mirror plane has no interaction with the TCNQ moieties; however, the hexamethylbenzene in the general position has an interaction as shown in Figure 6. This unsymmetrical interaction is distinctly different from that found in the 1:1 complex formed between hexamethylbenzene and TCNQ,[32] where the exo double bond of TCNQ is positioned above the center of the benzene ring. In this 1:1 complex[32] the interplanar distance between rings is 3.55 Å. In the present study the

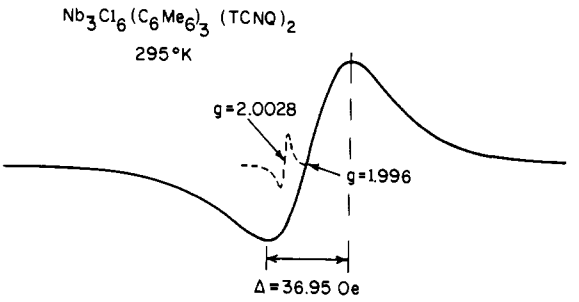

Figure 7. Room temperature ESR spectrum of 16.9 μmol of $Nb_3Cl_6(C_6Me_6)_3(TCNQ)_2$ (—) and pitch standard (3×10^{15} $S = ½$ spins) (- - - -).

nonplanarity of the hexamethylbenzene results in a rather large range of distances from the TCNQ plane (the ring carbons are 3.57–3.88 Å, mean 3.71 Å; the methyl carbons are 3.24–3.95 Å, mean = 3.65 Å). The least-squares plane through the benzene ring forms a dihedral angle of 3.52° with the TCNQ ring. Thus, there does not appear to be a very strong interaction between the arene coordinated and the TCNQ; the interaction is sufficient, however, to give rise to a novel crystal structure and a semiconducting behavior as discussed below.

Physical Measurements and Discussions

Two probe single-crystal and polycrystalline conductivities of $[Nb_3Cl_6(C_6Me_6)_3](TCNQ)_2$ were measured. Values of $\sim 1 \times 10^{-3}$ ohm^{-1} cm^{-1} [37] were obtained for single crystals (typically $0.3 \times 0.1 \times 0.05$ mm) along the needle axis (*a* axis) of the crystal. Polycrystalline samples[38] exhibited conductivities on the order of 15 times larger in value than that observed for single crystals. These data suggest the needle axis is not the highly conducting axis and that an axis of higher conductivity exists. This is consistent with the results of the structure determination, which indicate that the *b* axis should be the most highly conducting.

The temperature dependence of the conductivity exhibits a semiconductor behavior. Using the expression $\sigma = \sigma_0 e^{-E_a/kT}$, an activation energy E_a of 0.35 eV (2800 cm^{-1}) is found together with a $\sigma_0 = 0.4$ ohm^{-1} cm^{-1}. The room temperature conductivity is high for an alternating donor (cation)-acceptor (anion) system,[39] presumably due to the open-shell cation overlapping via the hexamethylbenzenes to the TCNQ dianionic dimer. The semiconducting behavior is consistent with the zig-zag structure of alternating cations and anions with an unpaired electron per repeat unit.

Differential scanning calorimetry traces reveal that $[Nb_3Cl_6(C_6Me_6)_3](TCNQ)_2$ is thermally stable below 150 °C. Above 150 °C exothermic decomposition is observed. An endothermic melting point was not observed.

The room temperature ESR spectrum of $Nb_3Cl_6(C_6Me_6)_3(TCNQ)_2$ in a polycrystalline sample consists of a relatively broad, nearly isotropic absorption. The *g* factor is 1.996 (2) and the peak to peak derivative line width is 36.95 (2) Oe as depicted in Figure 7. The *g* value indicates that the odd electron is localized on the Nb cluster, and the line width arises in part from inhomogeneous broadening due to unresolved hyperfine coupling in the solid state. The position below that of a free electron is also consistent with the ESR spectra reported for other niobium complexes. The Nb(II,III) complex $(Et_4N)_3(Nb_6Cl_{12})Cl_6$ [40,41] exhibits absorption at $g = 1.95$ (5) and a broad spectrum over 1000 Oe wide in the solid state. A variety of Nb(IV) complexes have also been reported to exhibit an ESR resonance at fields below the free electron values, e.g., $Nb^{IV}Cl_5(OR)^{2-}$ (R = Me, $\langle g \rangle = 1.861$ (2),[42] 1.903;[43] R = Et, $\langle g \rangle = 1.901$;[43] R = *i*-Pr, $\langle g \rangle = 1.902$[43]), $Nb^{IV}OX_4^{2-}$ (X

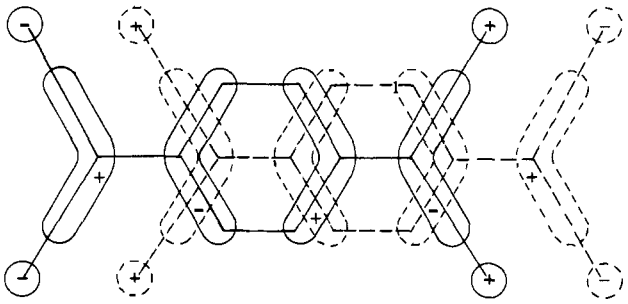

Figure 8. Schematic illustration of the bonding between $TCNQ_2^{2-}$. The filled a_g orbital arises from the overlap of the half-filled $2b_{2g}$ orbitals on isolated $TCNQ^-$ moieties. The signs of the wave functions of the top $TCNQ^-$ molecule (solid line) refer to the underneath side of molecular plane π lobes, while the converse is true for the underneath $TCNQ^-$ moiety (dashed line). The circles refer to the terminal N atoms.

= Cl, $\langle g \rangle$ = 1.944; X = F, $\langle g \rangle$ = 1.897 (6)),[44] and $Nb^{IV}O(acac)_2$ (acac = acetylacetonate, $\langle g \rangle$ = 1.944 (4)).[44] For these reasons we assign the odd electron in the $Nb_3Cl_6(C_6Me_6)_3(TCNQ)_2$ system to the trinuclear cluster, i.e., $[Nb_3Cl_6(C_6Me_6)_3]^{2+}(TCNQ)_2^{2-}$.[45] The nature of additional temperature-dependent line broadening mechanisms in the complex is currently being investigated. However, line width is clearly observed to increase with decreasing temperature.

The magnetic susceptibility at room temperature was determined by spin counting and comparison of the ESR spectrum of $Nb_3Cl_6(C_6Me_6)_3(TCNQ)_2$ to the pitch standard.[52] The nominal number of $S = \frac{1}{2}$ spins observed was 1.3×10^{19} for a 16.9-μmol sample. This is in good agreement with the assignment of two unpaired electrons per unit cell. Based on the dication formulation for the trimer we assigned a 2 − charge to the TCNQ dimer. This dianionic formulation agrees well with the observed structural data for the TCNQ moiety and represents the best structural characterization of an isolated $TCNQ^-$ dimer.

The highest occupied molecular orbital on each $TCNQ^-$ is the half-filled $2b_{2g}$ molecular orbital.[53-55] The $2b_{2g}$ orbitals interact upon dimer formation under C_{2h} symmetry to form a bonding a_g and an antibonding b_u orbital. The former, which is illustrated in Figure 8, is occupied by two or one electrons for the $(TCNQ^-)_2$ or $(TCNQ)_2^-$ formulations, respectively. The former formulation has a bond order of 1 as opposed to a bond order of $\frac{1}{2}$ for the latter case. This former situation is in accord with the observed short interplanar spacing of 3.10 Å.

From a consideration of the noble-gas rule there are four electrons used for metal–metal bonding as well as four nonbonding metal localized electrons associated with the monocationic cluster. Upon oxidation to the dication an electron is removed from a nonbonding orbital. Thus, the Nb–Nb distance reflects little change upon oxidation as Nb–Nb distance (3.335 (9) Å) is virtually equivalent to that reported for the monocation (3.334 (6) Å).[14] The mean Nb–Nb distance from the two independent Nb–Nb distances observed for the dication differs by greater than five standard deviations, suggesting a possible deviation from the equilateral framework reported for the monocation. Such a deviation upon oxidation is qualitatively reasonable in view of recent molecular orbital descriptions.[54] Metal–metal bond distances have also been shown in various cases to be insensitive to changes in bond order due to charge and packing effects.[55,56]

Acknowledgment. R.E., B.S., G.S., and S.Z.G. gratefully acknowledge the donors of the Petroleum Research Fund, administered by the American Chemical Society, for partial support of this work. J.S.M. and M.A. acknowledge the fruitful and stimulating discussions with Dr. A. J. Epstein.

Supplementary Material Available: a listing of structure factor amplitudes (14 pages). Ordering information is given on any current masthead page.

References and Notes

(1) (a) Department of Chemistry, University of Rochester; (b) Webster Research Center, Xerox Corporation.
(2) J. S. Miller and A. J. Epstein, *Prog. Inorg. Chem.*, **20**, 1 (1976), and references cited therein.
(3) H. R. Zeller, *Adv. Solid State Phys.*, **13**, 31 (1973).
(4) I. F. Shchegolev, *Phys. Status Solidi A*, **12**, 9 (1972).
(5) A. J. Heeger and A. F. Garito, *NATO Adv. Study Inst. Ser.*, **7**, 89 (1975).
(6) A. F. Garito and A. J. Heeger, *Acc. Chem. Res.*, **7**, 232 (1974).
(7) J. S. Miller, *Adv. Chem. Ser.*, **No. 150**, 18 (1976).
(8) W. A. Little, *Phys. Rev. A*, **134**, 1416 (1964); *Sci. Am.*, **212** (Feb.), 21 (1965); *NATO Adv. Study Inst. Ser., Ser. A*, **7**, 35 (1975).
(9) E. B. Yagubski and M. L. Khidekel, *Russ. Chem. Rev.*, **41**, 1011 (1972).
(10) D. S. Acker and D. C. Blomstrom, U.S. Patent 3162641 (1965).
(11) (a) L. R. Melby, R. J. Harder, W. R. Hertler, W. Mahler, R. E. Benson, and W. E. Mochel, *J. Am. Chem. Soc.*, **84**, 3374 (1962); (b) U. T. Muller-Westerhoff and P. Eilbracht, *ibid.*, **94**, 9272 (1972).
(12) (a) R. B. Shibaeva and L. O. Atovmyan, *J. Struct. Chem.*, **13**, 514 (1972); (b) F. H. Herbstein, *Perspect. Struct. Chem.*, **4**, 269 (1971).
(13) (a) R. P. Shibaeva, L. O. Atovmyan, and M. N. Orfanova, *Chem. Commun.*, 1494 (1969); (b) R. B. Lyubovsku, M. K. Makova, M. L. Khidekel, I. F. Shchegolev, and E. B. Yagubskii, *JETP Lett. (Engl. Transl.)*, **15**, 464 (1972).
(14) M. R. Churchill and S. W. Y. Chang, *J. Chem. Soc., Chem. Commun.*, 248 (1974).
(15) R. B. King, D. M. Braitsch, and P. N. Kapoor, *J. Chem. Soc., Chem. Commun.*, 1072 (1972).
(16) R. B. King, D. M. Braitsch, and P. N. Kapoor, *J. Am. Chem. Soc.*, **97**, 60 (1975).
(17) E. O. Fischer and F. Röhrscheid, *J. Organomet. Chem.*, **6**, 53 (1966).
(18) J. S. Miller and A. O. Goedde, *J. Chem. Educ.*, **50**, 431 (1973).
(19) "International Tables for X-Ray Crystallography", Vol. 1, Kynoch Press, Birmingham, England, 1969.
(20) The programs for refinement of lattice constants and automated as operation of the diffractometer are those of Busing and Levy as modified by Picker Corporation.
(21) T. C. Furnas, "Single Crystal Orienter Instrumentation Manual", General Electric Co., Milwaukee, Wis., 1957.
(22) S. Z. Goldberg, R. Eisenberg, J. S. Miller, and A. J. Epstein, *J. Am. Chem. Soc.*, **98**, 5173 (1976).
(23) S. Z. Goldberg, C. Kubiak, C. D. Meyer, and R. Eisenberg, *Inorg. Chem.*, **14**, 1650 (1975).
(24) All computations were carried out on an IBM 360/65 computer. Locally modified versions of the following programs were used: Raymond's URFACS for data reduction; Ibers' NUCLS, a group least-squares version of the Busing–Levy ORFLS program; Zalkin's FORDAP Fourier program; ORFFE, a function and error program by Busing, Martin, and Levy; Johnson's ORTEP2 thermal ellipsoid plotting program. A number of local programs were also used.
(25) D. T. Cromer and B. Mann, *Acta Crystallogr., Sect. A*, **24**, 321 (1968).
(26) D. T. Cromer and D. Lieberman, *J. Chem. Phys.*, **53**, 1891 (1970).
(27) $R_1 = \Sigma||F_o| - |F_c||/\Sigma|F_o|$; $R_2 = [\Sigma w(|F_o| - |F_c|)^2/\Sigma w|F_o|^2]^{1/2}$; estimated standard deviation of an observation of unit weight = $[\Sigma w(|F_o| - |F_c|)^2/(N_o - N_v)]^{1/2}$ where N_o and N_v are the number of observations and variables, respectively.
(28) See paragraph at end of paper regarding supplementary material.
(29) L. O. Brockway and J. M. Robertson, *J. Chem. Soc.*, 1324 (1959).
(30) M. F. Bailey and L. F. Dahl, *Inorg. Chem.*, **4**, 1298 (1965).
(31) G. Huttner, S. Lange, and E. O. Fischer, *Angew. Chem., Int. Ed., Engl.*, **10**, 556 (1971).
(32) R. H. Colton and D. E. Henn, *J. Chem. Soc. B*, 1532 (1970).
(33) P. Goldstein, K. Seff, and K. N. Trueblood, *Acta Crystallogr., Sect. B*, **24**, 778 (1968).
(34) A. Hoekstra, T. Spoelder, and A. Nos, *Acta Crystallogr., Sect. B*, **28**, 14 (1973).
(35) A. J. Epstein, N. O. Lipari, P. Nielson, and D. J. Sandman, *Phys. Rev. Lett.*, **14**, 914 (1975).
(36) (a) H. Kobayashi, T. Danno, and Y. Saito, *Acta Crystallogr., Sect. B*, **29**, 2693 (1973); (b) D. Chasseau, J. Gaultier, C. Hauw, and M. Schvoerer, *C. R. Acad. Sci., Ser. C*, **275**, 1491 (1972).
(37) Ohmic.
(38) J. S. Miller, *J. Am. Chem. Soc.*, **96**, 9131 (1974).
(39) D. J. Dahm, P. Horn, G. R. Johnson, M. G. Miles, and J. D. Wilson, *J. Cryst. Mol. Struct.*, **5**, 27 (1975).
(40) R. A. MacKay and R. F. Schneider, *Inorg. Chem.*, **6**, 549 (1967).
(41) The hyperfine splitting arising from the 100% natural abundance of $I = \frac{9}{2}$ ^{93}Nb is unresolved in solution, but not in the solid.
(42) P. G. Rasmussen, H. A. Kuska, and C. H. Brubaker, Jr., *Inorg. Chem.* **4**, 343 (1965).
(43) M. Lardon and H. H. Günthard, *J. Chem. Phys.*, **44**, 2010 (1966).
(44) I. F. Gainullin, N. S. Garifyanov, and B. M. Kozyrev, *Dokl. Chem.*, **180**, 497 (1967).
(45) One model of $Nb_3Cl_6(C_6Me_6)_3^+(TCNQ)_2^-$ requires the unpaired electron to reside in the a_g molecular orbital on the $(TCNQ)_2^-$. This model has been discarded, as the ESR signal should be typical of other TCNQ complex salts. The $TCNQ^{2-}$ resonances quinolinium$^+(TCNQ)_2^-$,[46] K^+TCNQ^-,[47]

Ph_3AsMe^+TCNQ,[48] and $(Cs^+)_2(TCNQ)_3^{2-}$ [49] occur at fields equal to or greater than that observed for the free electron and exhibit derivative peak to peak line width <5 Oe.[47,49]
(46) R. W. Tsien, C. H. Huggins, and U. H. LeBlanc, Jr., *J. Chem. Phys.*, **45**, 4370 (1966).
(47) J. P. Blanc, B. Cheminat, and H. Robert, *C. R. Acad. Sci., Ser. B*, **273**, 147 (1971).
(48) S. Braunsberger, H. Götz, and B. Walter, *Phys. Status Solidi A*, **15**, 69K (1973).
(49) D. B. Chesnut and P. Arthur, Jr., *J. Chem. Phys.*, **36**, 2969 (1962).
(50) C. P. Poole, Jr., "Electron Spin Resonance", Interscience, New York, N.Y., 1967, Chapter 20.
(51) J. Ladik, A. Karpfen, G. Stollhoff, and P. Fulde, *Chem. Phys.*, **7**, 267 (1975).
(52) A. Karpfen, J. Ladik, G. Stollhoff, and P. Fulde, *Chem. Phys.*, **8**, 215 (1975).
(53) N. O. Lipari, P. Nielsen, A. J. Epstein, and D. J. Sandman, submitted for publication.
(54) C. E. Strouse and L. F. Dahl, *Discuss. Faraday Soc.*, **47**, 93 (1969).
(55) C. E. Strouse and L. F. Dahl, *J. Am. Chem. Soc.*, **93**, 6032 (1971).
(56) L. F. Dahl, Abstracts, 165th National Meeting of the American Chemical Society, Dallas, Texas, 1973, No. INOR 6; Abstracts, 167th National Meeting of the American Chemical Society, Los Angeles, Calif., 1974, No. INOR 47; private communication.

Stereochemical Rigidity in ML_5 Complexes. 4. Preparations and Nuclear Magnetic Resonance Line-Shape Analyses of Intramolecular Exchange in Neutral ML_5 Complexes of Iron, Ruthenium, and Osmium

A. D. English,* S. D. Ittel, C. A. Tolman, P. Meakin, and J. P. Jesson

Contribution No. 2394 from the Central Research and Development Department, E. I. DuPont de Nemours and Company, Inc., Wilmington, Delaware 19898.
Received July 13, 1976

Abstract: A series of zerovalent d^8 ML_5 complexes has been synthesized (M = Fe, Ru, Os; L = phosphite). These novel species are characterized and their intramolecular exchange behavior is established by $^{31}P\{^1H\}$ NMR and a complete line-shape analysis. The intramolecular rearrangement barriers fall in the range of 7–9 kcal/mol. The variation of the rearrangement barrier as a function of the metal for the entire d^8 ML_5 series is defined by the present study and our previous work. The exchange processes and rearrangement barrier ordering are consistent with previous results for the cationic ML_5 species; therefore, the possibility of a dominant role for ion pairing in the previous studies is excluded.

Since the original work of Cotton and co-workers[1a] showing stereochemical nonrigidity in $Fe(CO)_5$, there has been considerable interest in defining the factors which influence barriers to intramolecular exchange in five-coordinate complexes. We have previously made extensive solution studies[2-6] of cationic d^8 ML_5 complexes; more recently we have turned our attention to the unknown zerovalent d^8 ML_5 species, where L is an alkyl phosphite. The $M(PF_3)_5$ complexes (M = Fe, Ru, Os) had been reported earlier by Kruck and Prasch.[7] While our work was in progress, Muetterties and Rathke independently reported the preparation of $Fe[P(OCH_3)_3]_5$ by sodium amalgam reduction.[8] We have described an NMR study of this complex in a communication,[9] and now wish to report the preparation and NMR behavior of the previously unknown $Ru[P(OCH_3)_3]_5$ and $Os[P(OCH_3)_3]_5$ complexes. We have also prepared $Fe[P(OC_2H_5)_3]_5$ and $Fe[P(O\text{-}n\text{-}C_3H_7)_3]_5$. This work permits a comparison of rearrangement barriers for the complete series of nine d^8 $M[P(OCH_3)_3]_5$ complexes, establishes a trigonal bipyramidal stereochemistry in all cases (from A_2B_3 patterns in the $^{31}P\{^1H\}$ NMR spectra), and confirms that ion pairing does not have a dominant role in the rearrangement process.

A detailed line-shape analysis of $Fe[P(OCH_3)_3]_5$ shows that there is simultaneous exchange of the pair of axial with a pair of equatorial ligands in the rearrangement process. This is the same permutation found in the cationic d^8 ML_5 species and is consistent with the Berry mechanism. The barriers to rearrangement vary from 7 to 9 kcal/mol for the three metals where the ligand is $P(OCH_3)_3$; the ordering is Fe > Ru < Os. This ordering is in agreement with previous results[5] on the isoelectronic cationic species. Intermolecular exchange does not occur for these complexes at an accessible temperature.

Results

A. Iron. The low-temperature limiting spectra have been obtained for three FeL_5 complexes. The complexes all have A_2B_3 patterns in the $^{31}P\{^1H\}$ NMR, indicating that the molecules have D_{3h} symmetry on the NMR time scale. The temperature-dependent spectra for two of the complexes have been analyzed and their rearrangement barriers calculated.

(i) **$Fe[P(OCH_3)_3]_5$.** This complex was prepared by sodium amalgam reduction of $FeBr_2$ in the presence of excess phosphite in a tetrahydrofuran solution. The product was purified by chromatography and the NMR data were obtained using pentane as the solvent.

The low-temperature limiting spectrum is obtained at −122 °C and is characteristic of a tightly coupled A_2B_3 spin system. The relevant NMR parameters are given in Table I.

A comparison of the observed spectrum of $Fe[P(OCH_3)_3]_5$ near the slow exchange limit with spectra calculated for the two possible types of permutational behavior in the rearrangement process is shown in Figure 1 at −104 °C. As with the cationic species,[5] behavior of type A (simultaneous exchange of two equatorial with the two axial ligands) gives a better fit at this, and other temperatures, than does behavior of type B (sequential exchange). The results are consistent with a Berry rearrangement[10] mechanism having a C_{4v} transition state.

Evidence for intermolecular exchange on the NMR time scale was sought using a solution of $Fe[P(OCH_3)_3]_5$ and $P(OCH_3)_3$ in benzonitrile. At temperatures of up to 140 °C no intermolecular exchange was apparent; the complex is stable for only a few minutes at this temperature.

(ii) **$Fe[P(OC_2H_5)_3]_5$.** This complex was prepared by a method